# E-eyes: Device-free Location-oriented Activity Identification Using Fine-grained WiFi Signatures

Yan Wang[†], Jian Liu[†], Yingying Chen[†], Marco Gruteser[*], Jie Yang[‡], Hongbo Liu[§]
[†]Stevens Institute of Technology, Hoboken, NJ 07030, USA
[*]Rutgers University, North Brunswick, NJ 08902, USA
[‡]Florida State University, Tallahassee, FL 32306, USA
[§]Indiana University-Purdue University Indianapolis, Indianapolis, IN 46202, USA
[†]{ywang48, jliu28, yingying.chen}@stevens.edu, [*]gruteser@winlab.rutgers.edu,
[‡]jie.yang@cs.fsu.edu, [§]hl45@iupui.edu

## ABSTRACT

Activity monitoring in home environments has become increasingly important and has the potential to support a broad array of applications including elder care, well-being management, and latchkey child safety. Traditional approaches involve wearable sensors and specialized hardware installations. This paper presents device-free location-oriented activity identification at home through the use of existing WiFi access points and WiFi devices (e.g., desktops, thermostats, refrigerators, smartTVs, laptops). Our low-cost system takes advantage of the ever more complex web of WiFi links between such devices and the increasingly fine-grained channel state information that can be extracted from such links. It examines channel features and can uniquely identify both in-place activities and walking movements across a home by comparing them against signal profiles. Signal profiles construction can be semi-supervised and the profiles can be adaptively updated to accommodate the movement of the mobile devices and day-to-day signal calibration. Our experimental evaluation in two apartments of different size demonstrates that our approach can achieve over 96% average true positive rate and less than 1% average false positive rate to distinguish a set of in-place and walking activities with only a single WiFi access point. Our prototype also shows that our system can work with wider signal band (802.11ac) with even higher accuracy.

## Categories and Subject Descriptors

H.4 [**Information Systems Applications**]: Miscellaneous

## Keywords

Channel State Information (CSI); WiFi; Activity Recognition; Device-Free; Location-Oriented;

## 1. INTRODUCTION

There exists a broad range of applications that benefit from higher-level contextual information—an understanding of activities that persons are engaged in, not just their position inside a coordinate system. For example, activity recognition is the essential part of a trend towards the quantified self. By tracking a sequence of meaningful activities and generating statistics for a person, it is possible to monitor well-being and suggest behavioral changes that improve health. Such activity tracking is arguably even more compelling for children and the elderly. In aging-in-place settings, it can be helpful to understand whether established routines are still followed since the absence of usual activities can be an important indicator for detecting falls and other situations of need.

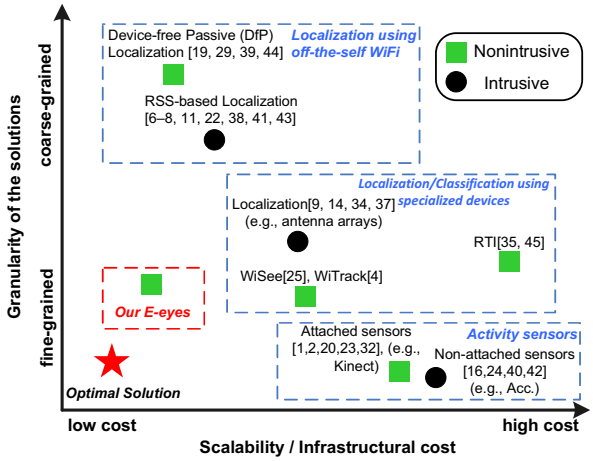


**Figure 1: Design Space: comparing to related work.**

**Existing solutions.** The challenge in activity recognition for these applications lies in finding solutions that can provide sufficiently accurate tracking and recognition with minimal infrastructure requirements and without the need to carry a dedicated device. As illustrated in Figure 1, existing activity recognition solutions [1, 2, 15, 16, 20, 23, 24, 32, 40, 42] primarily rely on dedicated sensors that are worn by the tracking subjects or cameras, motion sensors and other special sensors that are installed in the environment [1, 20, 32]. These solutions require either significant infrastructure installation or diligent usage of the wearable device. More generally, some activities that are tied to particular places can also be inferred from location systems [7, 44], either device-based or device-free, but these system cannot distinguish multiple activities that occur in the same place. Device-free systems do not require persons to carry any devices, but they require a dense placement of tens of sensors to create a mesh of wireless links inside the area of interest. Perhaps most related to our work is the effort to use detailed physical layer measurements such as Doppler shifts from one single wireless monitor to detect people's movement, location, and even gestures. The granularity of the monitoring ranges from coarser movements (such as Wi-Vi [5]) to fine-grained gestures (such as WiSee [25] and WiTrack [4]). However, these systems all have been prototyped with USRP software radios and require a specialized receiver that extracts carrier wave features that are not


*MobiCom'14,* September 7-11, 2014, Maui, Hawaii, USA.

http://dx.doi.org/10.1145/2639108.2639143.

reported in current WiFi systems. In addition, activity identification differs from gesture recognition in that the system needs to identify a more loosely defined series of motions over a period of time rather than a single well-defined body movement. For example, an activity such as cooking includes several movements to fetch, prepare, and mix ingredients that are not always exactly the same and do not necessarily occur in the same sequence, making it difficult to detect with gesture recognition techniques that are designed for precise single motions such as a punch.

**Approach.** This paper explores a novel point in the design space and demonstrates that device-free location-oriented activity recognition is possible (i) using the existing channel state information provided by IEEE 802.11n devices and (ii) using relatively few wireless links, such as those to existing in-home WiFi devices. The system exploits the trend to wider bandwidths (e.g., 802.11ac), and in particular, the more fine-grained channel state information that is being tracked in MIMO communications. Whereas traditional received signal strength (RSS) measurements are a single quantity per packet that represents signal-to-interference-plus-noise ratio (SINR) over the channel bandwidth, channel state information contains amplitude and phase measurements separately for each OFDM subcarrier. Due to the slight frequency delta, separate subcarriers experience different multipath fading. While such effects are often averaged out, when looking at a single average RSS measurement, the individual subcarrier measurements are more likely to change when small movements have altered the multipath environment. This essentially means that our system will not just detect obstructions on the direct path but can also take advantage of the rich web of reflected rays to cover a space. This makes it possible to operate with a single access point and a small set of stationary WiFi devices, which likely already exist or will exist soon in many buildings.

Moreover, many of the important daily activities that the device-free, location-oriented activity identification system (dubbed E-eyes) is designed to identify are linked to a few specific locations in the home, for example, cooking is usually limited to the kitchen and brushing teeth is limited to sinks. We seek therefore to identify activities from CSI signal measurement by comparing them to location-activity profiles. We also seek to distinguish two activities that occur in the same location, meaning that multiple location-oriented activity profiles can have the same location. We refer to this approach as location-oriented activity identification or as location-activity profiles, because the profiles are affected by both the activities that people perform and the location people are in. While traditional activity identification is more location independent [16, 42], our approach prioritizes device-free operation and detection of more loosely-defined daily activities involving a series of motions as opposed to gestures or basic sitting, walking, running classification. Our system can also be extended to recognize the same activity occurring in different locations by constructing multiple location-activity profiles for the same activity.

More specifically, our system first obtains wireless signals from off-the-shelf WiFi devices (e.g., Intel WiFi Link 5300 NICs) and classifies the wireless signals as belonging to an in-place or a walking activity. We refer these two types of activities as loosely-defined because they may involve non-repetitive body movements and the sequences of body movements involved may not remain the same across repetition. Examples of loosely-defined activities include cooking dinner in front of the stove, eating dinner at the dining table, exercising on a treadmill, or working at a desk. Walking activities involve movements between rooms or across a larger room. The system then applies novel matching algorithms to compare the amplitude measurements against known profiles that identify the activity. If known profiles do not exist or change afterwards, it can also apply semi-supervised learning strategies to establish or adaptively update profiles. Our system is device-free because it relies only on the existing WiFi environment (e.g., smart appliances connecting to a WiFi AP) and the person who performs the activities does not have to carry any device. This approach allows reusing the existing WiFi AP deployment in homes for location-oriented activity recognition, without the need for additional stationary infrastructure or wearable sensors. The contributions of our work are summarized as follows:

- We show that the channel state information (CSI) from off-the-shelf 802.11n devices can be utilized to identify and distinguish in-place activities inside a home with a much smaller set of transmitting devices than in previous device-free localization solutions.
- We develop a monitoring framework that can run on a single WiFi AP with its connected devices and use the associated profile matching algorithms to compare amplitude profiles against those from known activities.
- We explore dynamic profile construction. The profile can be adaptively updated to accommodate the movement or replacement of wireless devices (e.g., laptop or smartphone) and the day-to-day profile calibration.
- We conduct extensive experiments in two different-sized apartments over a 4-month time period to demonstrate that a single AP with 3 connected devices can accurately distinguish 8 walking activities between rooms (20 rounds each), 9 daily activities (50 rounds each), and over more than 100 rounds of other activities with an average detection rate of over 96% and an average false positive rate less than 1%. With only one device, the detection rate can still achieve around 92% with a similar false positive rate.
- We show through experiments how the trend to wider channels (e.g., 802.11ac) will further enhance recognition since it allows measurements over many additional subcarriers.

**Limitations.** Our system has the following limitations: first, our system E-eyes is mainly designed for and tested with a single occupant at home, which is an important scenario, such as in an aging-in-place environment. It may be extended to multiple persons, however this would require a much larger set of profiles covering different combinations of activities. Second, E-eyes was tested without pets or other movements at home. While the effect of small pets is probably negligible, larger pets may pose additional signal processing challenges. Third, E-eyes relies on a relatively stable environment (e.g., no furniture movement). While it could detect such environment changes, each would trigger an activity profile updating procedure, which may require user input.

The rest of the paper is organized as follows. In Section 2, we place our work in the context of related research. The background, challenges, and system overview of E-eyes are provided in Section 3. In Section 4, we present the proposed activity recognition schemes. We then describe the implementation of E-eyes in Section 5. In Section 6, we perform extensive evaluation of our system in real environments with two apartments. The related issues of E-eyes are discussed in Section 7. Finally, we conclude our work in Section 8.

## 2. RELATED WORK

There has been active work in using dedicated sensors for activity recognition [1, 2, 15, 16, 20, 23, 24, 32, 40, 42]. Sensors can be either attached to a person's body [16], or placed on target objects with which people interact [15]. For example, an accelerometer

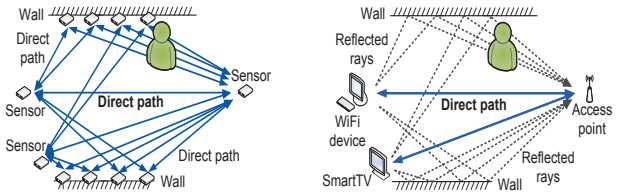


(a) Existing work: link-centric using RSS (b) Illustration of reflected rays

**Figure 2: CSI takes the advantage of multipath effects and captures the detailed changes on different subcarriers.**

is attached on human body to detect falls in Philips Lifeline [24], whereas a motion sensor is attached to a door to detect movement in GrandCare [32]. Another wearable sensor is the acoustic sensor used in BodyScop for classifying activities, such as eating and coughing [42]. Vision based systems [1, 20], such as Leap [2] and Kinect [23], can be used to track user movements and gestures. These dedicated sensors can achieve fine-grained activity recognition. However, they need the installation and maintenance of dedicated sensors which usually entail high costs and are thus not scalable.

Another body of related work is indoor localization systems which can be extended to activity recognition [6–9, 11, 14, 17, 21, 22, 30, 34, 37, 38, 41, 43]. These systems localize a wireless emitter using Received Signal Strength (RSS) [6–8, 11, 17, 22, 38, 41, 43], OFDM channel state information [30], antenna arrays [14,37], RFID tags [34], rotating anchors [9], or visible LED lights [21]. These systems provide various accuracy ranging from several meters (e.g., RSS-based) to sub-meter but require people to carry a wireless emitter. This can be intrusive and poses the problem of people, especially the elderly with age-related memory loss, forgetting to carry such a device. Furthermore, they need the support of wireless infrastructure, either lightweight devices such as re-use multiple access points if available [7, 11, 22] or costly specialized devices, such as antenna arrays [14, 37]. The infrastructural cost of these systems thus prevents their large scale deployment.

The radio tomography imaging (RTI) [35, 45] and device-free passive (DfP) localization [19, 29, 39, 44], like our system, do not require a device be attached to or carried by the user. The state of art RTI requires tens or hundreds of wireless sensors to achieve sub-meter accuracy, while DfP localization [19, 29] with four WiFi APs has an accuracy of several meters. Several works [13, 31] propose to distinguish some basic activities such as walking, crawling, standing and lying based on RSS using a set of receivers or USRP SDR devices. These systems are either impractical for roaming deployment or not accurate enough for fine-grained activity recognition.

Recent work in using a single wireless monitor to detect human movement or location [4, 5, 25] can be used for activity recognition as well. The granularity of the activity can be inferred from these systems is either modest (such as Wi-Vi [5]) or fine-grained (such as WiSee [25] and WiTrack [4]). However, these systems all require a specialized WiFi monitor (e.g., USRP) for extracting the carrier wave. In contrast, we use an off-the-shelf WiFi device for activity recognition. Our method can provide fine-grained activity recognition by re-using existing home WiFi network and thus has much higher scalability for wide deployment. Furthermore, different from WiSee that focuses on recognizing well-defined, quick gestures, our work aims to discriminate loosely defined daily activities that involve a series of body movements over a certain period of time. In recognizing such loosely defined daily activities, we find that channel characteristics, such as the statistical distribution and time series, are more suitable for distinguishing between activities lasting a certain period of time than quick gestures.

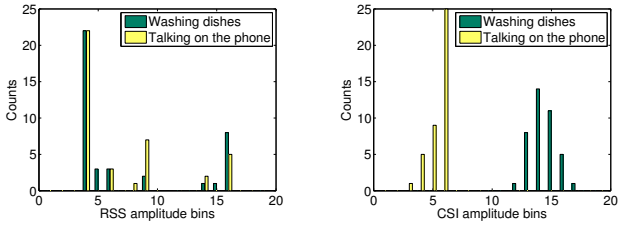


(a) RSS distribution (b) CSI distribution

**Figure 3: Histograms of RSS amplitude and CSI amplitude of a particular subcarrier for two different in-place activities at the same position: washing dishes and talking on the phone nearby the sink.**

# 3. DESIGN OF E-EYES

To build a low-cost solution leveraging WiFi signatures in a home environment, we devise an approach that senses and identifies fine-grained WiFi signal changes when an activity is performed. In this section, we discuss the intuition, challenges and overview of our system design.

## 3.1 Intuition

This work seeks to exploit two trends. First, WiFi usage has expanded from providing laptop Internet connectivity to connecting smart devices such as TVs, game consoles, surveillance cameras, refrigerators, and loudspeakers to home networks and the Internet. This provides a larger number of WiFi links inside homes, some of which use constant beaconing. Second, WiFi radios provide more fine-grained channel measurements over wider bandwidths. With 802.11n MIMO systems, it became necessary for radios to track more fine-grained channel state information. On it's standard 20MHz channel, 802.11n radios measure amplitude and phase for each of the 52 orthogonal frequency-division multiplexing (OFDM) subcarriers. With 40MHz channels, measurements are available for 128 subcarriers. The emerging IEEE 802.11ac standard supports even wider bandwidths. These measurements essentially allow estimating the channel frequency response. In contrast, the traditional received signal strength (RSS) was only a single value per packet, typically a SINR reading averaged over the entire channel bandwidth.

Measuring the channel frequency response has important implications for detecting and differentiating minute movements. Inside buildings, signal propagation is dominated by multipath, that is the received signal amplitude (or strength) is the combined amplitude of signals arriving over many different paths (scattered from and reflected off different objects). Since the individual signals can constructively or deconstructively, combine based on their individual phase shifts, this effect can lead to large differences in the combined amplitude, which is commonly known as small-scale fading. A small change in frequency, however, can have a large effect on the combined signal. The amount of frequency change for a signal amplitude to become uncorrelated with its previous value is also known as the coherence bandwidth and can be estimated as $B_c = \frac{1}{D}$ where $D$ is the delay spread of the arriving multipath signals. Interestingly, the width of an OFDM subcarrier is chosen to match this coherence bandwidth to simplify receiver design. This means that amplitude measurements on each subcarrier will provide many uncorrelated combinations of the received multipath components, which increases the likelihood that some are affected by a small movement. A single RSS measurement over the signal bandwidth, in comparison, averages out many of these detailed small scale fading effects.

Figure 3 shows a motivational experiment where two different activities were conducted in the same location: talking on the phone

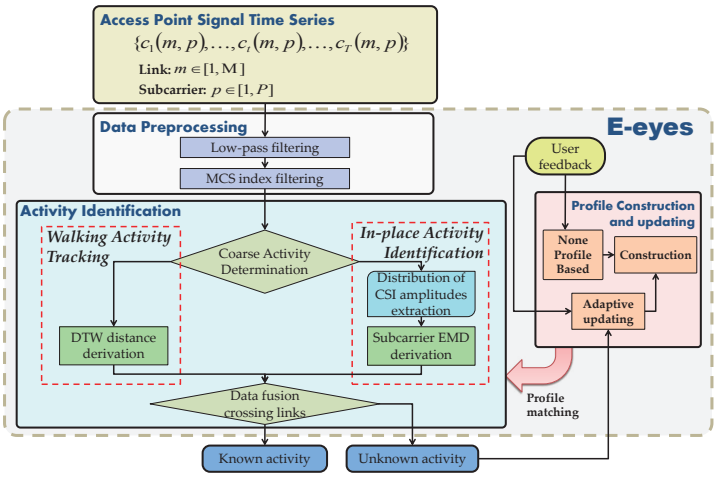


**Figure 4: System flow of activity recognition using CSI.**

and washing dishes. The histograms of RSS readings collected for both of these activities show relatively little difference. The histograms of CSI amplitudes (quantized to 20 bins) for a specific subcarrier, however, show very distinct distributions that can clearly distinguish these different movements in the same location. The insight is that since an activity involves a series of body movements during a certain period of time, the distribution of CSI amplitudes is a desirable channel statistic that can capture unique characteristics of activities in both time and frequency domains.

With more WiFi devices in homes and the ability to measure small changes in multipath rays, our intuition suggests that it might be possible to track activities and movements around a home with only this existing infrastructure. Device-free localization and activity recognition requires that at least one measurable RF rays travels through any location of interest, because the presence or movement of a human body at this position would only alter the propagation of these rays. Earlier device free localization system have therefore blanketed spaces with tens of transceivers to create a fine mesh of measurable direct links. As illustrated in Figure 2(a) and (b), such a measurable mesh can now also be created by all the multipath rays from only a handful of WiFi devices instead of requiring many additional devices.

## 3.2 Challenges

Realizing such a system that seeks to recognize activities at an access point using CSI measurements from only a small number of WiFi links raises a number of challenges:

**Profile Uniqueness and Robustness.** CSI measurements can be affected by signal interferences, user movements, and changing environments. To identify activities, the system has to match signatures or features of activities to measurements in a way that is robust to noisy signal readings collected from WiFi devices in real-world environments yet are still sufficiently unique to map to a specific activity.

**Algorithm Generality.** Distinguishing different activities needs different information of activities. For example, one activity might involve walking from one room to another (which generates a time series of CSI measurements without an obvious pattern), whereas another activity (e.g., washing dishes in the kitchen) is only performed at one location with repetitive gestures (which results in CSI measurements with repetitive patterns). These different types of activities will lead to very different signal characteristics, and our algorithm should be general enough to profile and identify them.

**Profile Generation.** After system installation or after significant changes to the environment, appropriate profiles for activities may not exist. The system should be able to assist with profile generation, to reduce the effort of this process.

## 3.3 System Overview

The basic idea of our system is to match CSI patterns against activity profiles. As illustrated in Figure 4, the system takes as input time-series amplitude measurements, which can be collected at a single access point with off-the-shelf hardware (e.g., Intel 5300 NIC). The amplitude measurements are available for each subcarrier on a link and are collected over several links to rarely moved devices (such as home entertainment devices or appliances). We discuss later on how the system might be extended to also take advantage of mobile devices when they do not move. The system can take advantage of CSI measurements from existing traffic across these links, or if insufficient network traffic is available, the system might also generate periodic traffic for measurement purposes. This data is then preprocessed to remove outliers via a low-pass filter and to filter out artifacts introduces by rate adaptation, where the radios switch to different modulation and coding schemes.

The core of our system, E-eyes, are the *Activity Identification* and the *Profile Construction and Updating*. Activity identification encompasses two different activity matching approaches to address the generality challenge. The system distinguishes between walking activities and in-place activities. In general, a walking activity causes significant pattern changes of the CSI amplitude over time, since it involves significant body movements and location changes. An in-place activity (such as watching TV on a sofa) only involves relative smaller body movements and will not cause significant amplitude changes but present certain repetitive patterns. It thus first applies a moving variance thresholding technique to discriminate the two types of activities. The cumulative moving variance across all subcarriers can be expected to be greater for walking activities than in-place activities. Moreover, our system leverages the moving variance to segment the long-term CSI trace. Since the trace often contains multiple different activities over time, moving variance is used to determine the start and end of individual activities.

Next, our system identifies activities by calculating the similarity between such a CSI segment and the pre-constructed activity profiles. Based on the characteristics of walking and in-place activities, we develop two separate similarity metrics and classifiers. For walking activities, we use the *Multiple-Dimensional Dynamic Time Warping (MD-DTW)* technique, which can align a trace with larger CSI changes to the profile while correcting for differences in speed. For in-place activities, we base the comparison on CSI distributions (i.e., histograms) rather than the exact time series to

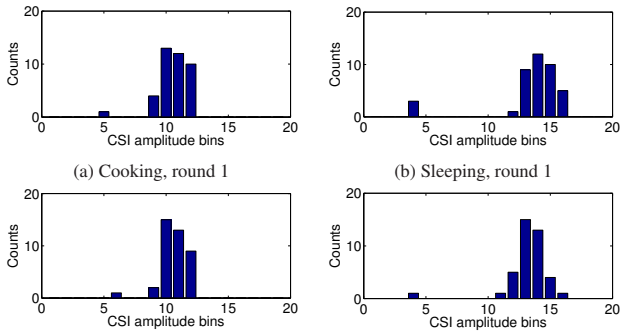


(a) Cooking, round 1 (b) Sleeping, round 1

(c) Cooki ng, round 2 (d) Sleeping, round 2

**Figure 5: Histogram of CSI amplitudes on a particular subcarrier for cooking and sleeping.**

achieve higher robustness to the repetitive but often more random patterns generated by such activities. We use the *Earth Mover Distance (EMD)* to quantify the similarity of two distributions.

To construct activity profiles, our system can utilize a semisupervised approach. It starts with continuous monitoring of a home environment and applies a clustering-based method to identify multiple similar instances of an activity without a matching profile (referred to *non-profile based*). Users can then label the resulting clusters to create known activity profiles. Furthermore, this technique can be used to detect and update activity profiles after significant changes in the environment (e.g., the media console WiFi device has been moved from one side of the room to the other side or the furnishings have been significantly altered). Users can provide feedback and trigger a profile update (after such environmental changes) by using the Non-profiling Clustering (Section 5.2).

# 4. ACTIVITY IDENTIFICATION

In this section, we first describe *Coarse Activity Determination*. We then present *In-place Activity Identification* and *Walking Activity Tracking* components in our system. And we also discuss how our system can benefit from wider signal bandwidths using 802.11ac.

## 4.1 Coarse Activity Determination

Since various activities cause different degrees of signal changes, we apply the *moving variance* on top of the CSI measurements to capture this difference and determine the category of the activity. In particular, a large moving variance indicates the presence of a walking activity whereas a small moving variance represents the presence of an in-place activity or no activity at all. The detailed steps are presented as follows:

**Step 1.** We denote the CSI samples of $P$ subcarriers as $C = \{C(1), \ldots, C(p), \ldots, C(P)\}$, where $C(p) = [c_1(p), \ldots, c_T(p)]'$ represents $T$ CSI amplitudes on the $p^{th}$ subcarrier. We further denote the moving variances of the $P$ subcarriers as $V = \{V(1), \ldots, V(p), \ldots, V(P)\}$, where $V(p) = [v_1(p), \ldots, v_T(p)]$ are the moving variances derived from $C(P)$. Our system can then calculate the *cumulative moving variance* of CSI samples crossing $P$ subcarriers as $\mathcal{V} = \sum_{p=1}^{P} V(p)$.

**Step 2.** The next step is to examine the cumulative moving variances to determine whether the collected CSI samples contain a walking activity or an in-place/no activity. If the maximum cumulative moving variance $\max(\mathcal{V})$ is larger than the threshold $\tau_v$, the CSI samples are determined to contain a walking activity, otherwise they contain an in-place/no activity. We empirically determine the threshold through 40 rounds of different walking activities and in-place activities in apartment environments. A threshold, $\tau_v = 20$, is found to be able to distinguish over 98% of walking and in-place activities in our experiments.

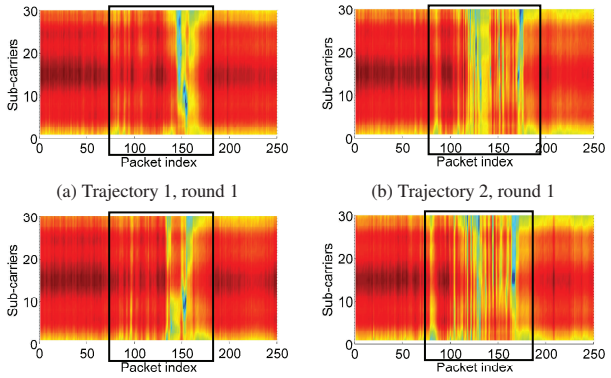


(a) Trajectory 1, round 1 (b) Trajectory 2, round 1

(a) Trajectory 1, round 2 (b) Trajectory 2, round 2

**Figure 6: Similar CSI time series pattern for same walking trajectory.**

Compared with recognizing gestures, people's daily in-place activities do not have such strictly pre-defined patterns but result in a relatively stable distribution of CSI amplitude due to the presence of the human body and loosely defined body motions. In E-eyes, segmentation is first performed in the task of Coarse Activity Determination by examining the CSI variance in the collected trace. Note that Coarse Activity Determination can be also used to identify the starting and ending of both walking activities and in-place activities, since walking activities often separate in-place activities. If the segmented CSI trace belongs to an in-place activity, we will further use the EMD technique [28] to compare the distribution of CSI amplitudes in a sliding time window with in-place activity profiles (Section 4.2) to identify different activities within this trace. If the segmented CSI trace is recognized as a walking activity, we will further identify the walking trajectory or the passing of doorways (Section 4.3).

## 4.2 In-place Activity Identification

### 4.2.1 Characteristics

We find that an in-place activity results in a relatively stable distribution of CSI amplitude due to the presence of the human body and (possibly) repetitive body movement over time. Furthermore, different in-place activities cause different distributions of CSI amplitude as the location and/or the repetitive body movement patterns and the posture of the human body are different for different in-place activities. We illustrate the similarity of the CSI amplitude distribution for the same activity, and the difference of the CSI amplitude distribution for two different in-place activities (i.e., cooking in a kitchen and sleeping on a bed) at a particular subcarrier (subcarrier 12) in Figure 5. We observe that the CSI amplitude distributions are similar for the same activity at different rounds, but distinctive for different activities. This important observation inspires us to exploit the distribution of CSI amplitude to distinguish different in-place activities and shows that a particular in-place activity can be identified by comparing against known profiles.

### 4.2.2 In-place Activity Classifier

Based on the characteristics of the in-place activities, we employ the earth mover's distance (EMD) [28] technique, which is a well-known approach for evaluating the similarity between two probability distributions. The EMD calculates the minimal cost to transform one distribution into the other. Our classifier seeks to compare the distribution of the testing CSI measurements to those of the known in-place activity profiles by using the EMD metric. CSI measurements being tested are identified to contain a known activity when the resulted minimal cost (i.e., minimal EMD distance) is small enough.

Specifically, at run time, our system first identifies the testing CSI measurements as a *candidate* of a particular known in-place activity if the EMD distance from the candidate to the known in-place activity is the minimum among the EMD distances to all known activities stored in the CSI profiles. Then our system further confirms the candidate known in-place activity by comparing the resulted minimal EMD distance to a threshold, which can be empirically determined in the profile construction. The candidate known in-place activity is confirmed if the minimal EMD distance is less than the threshold, otherwise, it will be identified as an unknown activity. An alternate way to determine whether the testing CSI measurements correspond to a known activity or not is to use an outlier detection method, such as the median absolute deviation (MAD) [27], to examine whether the resultant minimum EMD distance is within a range. To determine the range, an EMD distance pool containing the minimal EMD distances of previous successfully identified activities is needed in the profiles. We note that our system can also recognize the same in-place activities occurring in different locations by comparing the testing CSI measurements to a set of CSI profiles constructed when the same activities occur in different locations. In this case, the profile for an activity is a set of CSI profiles instead of a single CSI profile, and the testing CSI measurements are determined to contain the activity if it has the minimum EMD distance to any of the CSI profiles belonging to the activity profile.

## 4.3 Walking Activity Tracking

### *4.3.1 Characteristics*

We find that the CSI collected from walking activities is changing constantly over time due to body movement and change of locations. In particular, Figure 6 presents CSI amplitude of each subcarrier versus the packet index (i.e., time series) for two different walking paths in two experimental runs. We observe that the CSI measurements exhibit similar changing patterns for the same trajectory in different rounds, whereas the changes of CSI measurements over time are different for different trajectories. This observation indicates that the CSI pattern is dominated by the unique path of each walking activity.

Furthermore, since there are always in-place activities before and after a walking activity, ideally we can identify the walking activity by identifying the in-place activities at both ends. However, the starting and ending points of the walking activity can be anywhere inside the space. It is possible that the two endpoints are not that meaningful and thus no such in-place activity profiles are constructed. To tackle this problem, we propose to further build the CSI measurement profile when the person passes through doorways. Since, in general, a person must pass through a door way when walking from one room to another, they can be utilized to facilitate walking activity tracking. By identifying the doorway the person moves through, our system can determine a walking activity in high level without requiring extensive profiling of paths that have less meaningful starting and ending locations.

### *4.3.2 Walking Activity Discrimination*

**Walking Path Discrimination.** Since people may walk at different speeds for the same trajectory, we propose using Dynamic Time Warping (DTW) [26] to align the testing CSI measurements to those of known activities in the profile. We then identify the activity contained inside the testing CSI measurements based on the similarity measures using DTW. DTW stretches and compresses required parts to allow a proper comparison between two data sequences. This is useful to match CSI samples from different walking speeds in real-world scenarios. In our system, CSI measurements are in a format that reports the channel metrics for multiple subcarrier groups (e.g., 30 subcarriers). To perform multi-dimensional sequence alignment, our system employs Multi-Dimensional Dynamic Time Warping (MD-DTW) [33], in which the vector norm is utilized to calculate the distance matrix according to:

$$d(c_i, c'_j) = \sum_{p=1}^{P} (c_i(p) - c'_j(p))^2, \quad (1)$$

where $C = c_1, c_2, ..., c_T$ and $C'$=$c'_1, c'_2, ..., c'_T$ are two CSI sequences for walking path discrimination, and where $P$ is the number of dimensions of the sequence data (with $P$=30 for CSI sample). A least cost path is found through this matrix and the MD-DTW distance is the sum of matrix elements along the path.

During activity identification, our system distinguishes each walking activity by calculating the MD-DTW distance between the testing CSI measurements and all the known walking activities in CSI profiles. Our system stores the segment of CSI measurements of known activities in profiles. If the MD-DTW distance is less than a threshold (i.e., considering it as a known activity), we then regard the corresponding CSI measurements labeled in the CSI profiles with the minimum distance as the activity identified for the testing measurements.

**Doorway Discrimination.** Doorway discrimination is used to handle the case where the testing CSI measurements are unknown after attempting to match them with the profile database. We seek to identify which doorway the person passes through and the corresponding walking activity can then be recognized in a high-level. This strategy makes our system more robust and handles the case when people are moving freely. The possible activities are strongly tied to which doorway the person passes by. For example, passing through kitchen doorway in the noon time is very likely followed by cooking or eating.

In particular, our system also collects CSI for profiling when people pass through doorways during walking activity profile construction (i.e., constructing doorway profiles). It then compares the testing CSI measurements using a sliding window approach to that of the doorway profiles. The EMD distance used in in-place activity recognition is applied for such comparison. Therefore, distinguishing between passing different doorways is transformed into an in-place activities identification. To show the feasibility of this strategy, we test 20 rounds each for 8 walking trajectories (refer to Figure 7) in two different-size apartments. Table 1 shows the doorway detection ratio (DR) of each trajectory corresponding to the doorway passed. Our approach achieves an average detection accuracy of over 96.25%, which is sufficient as a supplementary to walking trajectory discrimination.

## 4.4 Extension to Wider-band WiFi Signals

The direction of WiFi protocol development moves towards extending the channel capacity and data transmission rate. A very efficient way to achieve the extension is to use wider-band channels, for example 802.11n protocol has the option to use 40MHz channels to increase the data rate from 54Mbits/s to 150Mbits/s per spatial stream. Similarly, the next generation WiFi protocol 802.11ac would support 80MHz and 160MHz channels with the data rate up to 867Mbits/s per spatial stream. The increasing trend of the channel bandwidth also brings us more available subcarriers in each channel (i.e., 114 subcarriers for a 40MHz channel,

**Table 1: Doorway Detection Accuracy.**

| 1-BR Apt. | Bedroom↔Kitchen | Kitchen↔Bathroom |
|---|---|---|
| DR | 1 | 0.975 |
| 2-BR Apt. | Outside↔Bedroom1 | Bedroom2↔Bathroom |
| DR | 1 | 0.875 |

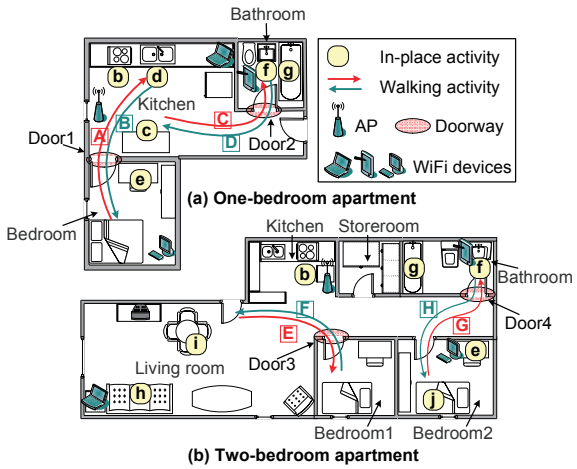


**Figure 7: Experimental setups and the illustration of activities in two different-size apartments: (a) one-bedroom apartment and (b) two-bedroom apartment.**

242 subcarriers for a 80MHz channel), which suggests that using wider-band signals could potentially increase the performance of activity recognition using CSI measurements since more subcarriers available in CSI would increase the chance to capture the detailed small-scale fading effects caused by small activities. In this direction, we seek to extend E-eyes to use a wider-band signal providing CSI measurements with more subcarrier information which is expected to help improve the activity recognition accuracy especially for in-place activities. We utilize two 40MHz channel in 802.11n to emulate an 80MHz channel in 802.11ac in our experiments.

# 5. IMPLEMENTATION

## 5.1 Activity Profile Construction

In our system, we collect the CSI measurements of typical activities for profile construction. In particular, we use the distribution of CSI amplitude to profile in-place activities and the sequence of CSI amplitude for walking activities. If multiple WiFi devices are available, the profile is constructed by using each WiFi device. Additionally, we build a profile for "empty room" (i.e., no one inside the room), which is a special case of an in-place activity. When constructing profiles, it is possible the profile of an activity from a particular WiFi device is similar to the profile of "empty room" when the activity is very far away from that device.

## 5.2 Non-profiling Clustering

After profile construction, the activity profiles may still change due to many factors. For example, the activity profiles may change over time due to the involved WiFi device being moved to another location, e.g., the desktop being moved from one room to another. Furthermore, the activity profiles may also get affected by day-to-day environmental changes. Therefore, our system E-eyes requires a method that can adaptively update activity profiles. We propose a process called *non-profiling clustering*, in which E-eyes first utilizes a semi-supervised approach to cluster the daily activities from the collected CSI measurements, and then label each activity to produce CSI profiles. After clustering, the CSI measurements from the same type of activities are clustered together. Once significant changes of profiles are detected, E-eyes utilizes users' feedback (i.e., user labels each new cluster returned by non-profile clustering) to perform adaptive profile updating. The non-profiling clustering is also utilized to construct CSI profiles when our system starts without any CSI profile.

We next illustrate this strategy by applying clustering to profile in-place activities. Assume we have $R$ sets of CSI samples from $K$ different unknown activity instances, where each CSI sample set $C^r, 1 \leq r \leq R$, corresponds to one particular activity instance with a certain number of CSI samples. Here we exploit the K-Means clustering technique to discriminate different activity instances based on the EMD between CSI samples.

In order to utilize EMD for clustering, we first calculate the EMD between any particular CSI sample set $C^r$ and all the sample sets (including $C^r$ itself). We then obtain $R$ EMD vectors of length $R$, i.e., $E^r = \left[E(C^r, C^1), \cdots, E(C^r, C^R)\right]$. Next, the K-means algorithm searches for $K$ appropriate clusters, i.e., $S = s_1, \cdots, s_K$, satisfying the following equation:

$$\arg\min_{S} \sum_{k=1}^{K} \sum_{E^r \in s_k} |E^r - \mu_k|^2, \quad (2)$$

where $\mu_k$ is the mean value of the EMD vectors in $s_k$. Equation 2 searches for $K$ appropriate clusters $S$ that minimizes the variances of the CSI vectors $C^r$ in each cluster.

Table 2 shows the results of clustering based on 400 CSI sample sets involving 8 activity instances, where each set contains 40 CSI samples. Most of the activities can be differentiated from each other with the detection ratio as high as over 84% and an acceptable false positive rate, except the two activities of brushing and bathing in the bathroom due to the small differences in their corresponding CSI patterns, which cannot be differentiated by clustering.

With the relationship between the activity instances and the clusters $S$, the CSI sample sets correctly classified are used to create new activity profiles. Furthermore, if the profile for a particular activity instance already exists, the system adaptively determines whether to update the activity profile through the comparison with the new profile.

## 5.3 Data Calibration

Data calibration is used to improve the reliability of the CSI by mitigating the noise presented in the collected CSI samples. The noise sources could be the complicated indoor propagation, the WiFi devices' inner noise (e.g., vibration or ring of devices), and etc.

### 5.3.1 *Low-pass Filtering*

Low-pass filtering aims to remove high frequency noise which is unlikely to be caused by human activities as human activities usually have a low frequency range. To remove high frequency noises, we adopt the dynamic exponential smoothing filter (DESF) [10], since it is an exponential smoother that changes its smoothing factor dynamically according to previous samples. The DESF can remove high frequency noise and preserve the features affected by human activities in the CSI measurements.

### 5.3.2 *Modulation and Coding Scheme Index Filtering*

Besides the effects from human activities, we find that the modulation and coding scheme (MCS) index, which occasionally changes due to the unstable wireless channel in our experiments, could also influence the amplitude of CSI. To get the changing CSI patterns only affected by human activities, we need to remove the CSI mea-

**Table 2: Results of activity identification using clustering without profiles.**

| Test | empty $s_1$ | cook. $s_2$ | eat. $s_3$ | wash. $s_4$ | study. $s_5$ | brush. $s_6$ | bath. $s_7$ | other $s_8$ |
|---|---|---|---|---|---|---|---|---|
| DR | 1 | 0.98 | 0.88 | 0.84 | 0.92 | 0.66 | 0.46 | 0.94 |
| FPR | 0.06 | 0 | 0.15 | 0.09 | 0 | 0.45 | 0.43 | 0.10 |

| Actual Activity Performed \ Identified In-place Activity | a | b | c | d | e | f | g | unknown |
|---|---|---|---|---|---|---|---|---|
| a: empty | 1 | 0 | 0 | 0 | 0 | 0 | 0 | 0 |
| b: cooking | 0 | 1 | 0 | 0 | 0 | 0 | 0 | 0 |
| c: eating | 0 | 0 | 1 | 0 | 0 | 0 | 0 | 0 |
| d: washing dishes | 0 | 0 | 0.16 | 0.84 | 0 | 0 | 0 | 0 |
| e: studying | 0 | 0 | 0 | 0 | 1 | 0 | 0 | 0 |
| f: brushing | 0 | 0 | 0.06 | 0 | 0 | 0.94 | 0 | 0 |
| g: bathing | 0 | 0 | 0.02 | 0 | 0 | 0 | 0.98 | 0 |
| o: others | 0 | 0 | 0 | 0 | 0 | 0 | 0 | 1 |

(a) 1-bedroom apartment

| Actual Activity Performed \ Identified In-place Activity | a | b | f | g | h | i | j | unknown |
|---|---|---|---|---|---|---|---|---|
| a: empty | 1 | 0 | 0 | 0 | 0 | 0 | 0 | 0 |
| b: cooking | 0 | 1 | 0 | 0 | 0 | 0 | 0 | 0 |
| f: brushing | 0 | 0 | 1 | 0 | 0 | 0 | 0 | 0 |
| g: bathing | 0 | 0 | 0 | 0.96 | 0 | 0 | 0 | 0.04 |
| h: watching TV | 0 | 0 | 0 | 0 | 1 | 0 | 0 | 0 |
| i: gaming | 0 | 0 | 0 | 0 | 0 | 1 | 0 | 0 |
| j: sleeping | 0 | 0 | 0 | 0 | 0 | 0 | 0.88 | 0.12 |
| o: others | 0 | 0 | 0 | 0 | 0 | 0 | 0.05 | 0.95 |

(b) 2-bedroom apartment

**Figure 8: Confusion matrix of in-place activity identification in two different apartments.**

surements affected by a different MCS index (indicates different channel condition) for a pure reflection metric of human activities.

Specifically, MCS index is a specification of the high-throughput (HT) physical layer (PHY) parameter in 802.11n standard [3]. It contains the information of the modulation order (e.g., BPSK, QPSK, 16-QAM, 64-QAM), the forward error correction (FEC) coding rate, etc. for transmitting a packet. Each 802.11n packet header contains a 16-bit MCS index, which can be extracted together with the CSI sample of each packet. In particular, we find that CSI measurements with the MCS index greater than 263 [1] can make CSI measurements relatively stable in empty rooms even though it changes in such a range. Therefore, we filter out the CSI measurements with MCS value less than 263 and keep the rest of them for activity identification.

## 5.4 Data Fusion Crossing Multiple Links

WiFi usage has expanded from providing Internet access to connecting in-home smart devices such as TVs, refrigerators, and loudspeakers. This provides a number of WiFi links to capture an activity simultaneously inside home. Our system E-eyes thus can exploit a number of WiFi links to improve the activity recognition accuracy based on the basic schemes shown in Section 4.

Assume we have $L$ WiFi devices collecting CSI measurements independently and each device has $J$ activity profiles denoted as $\{a_1^l, \ldots, a_j^l, \ldots, a_J^l\}, l = 1, \ldots, L$. The final activity recognition result is the $j^{th}$ activity (profile) that minimizes the weighted summation of the similarities between the collected CSI measurements and the profiles on each WiFi device, i.e.,

$$a_j^* = \arg\min_j \sum_{l=1}^{L} [w_j^l(a_0^l, a_j^l) \times D_j^l], \quad (3)$$

where $D_j^l$ is the EMD or DTW distance (Section 4.2.1 and 4.3) between the CSI measurements and the $j^{th}$ activity profile on the $l^{th}$ WiFi device; $w_j^l(a_0^l, a_j^l)$ is the normalized weight dominated by the significance of the $j^{th}$ activity on the $l^{th}$ WiFi device, which is defined as follows:

[1]The MCS index of 263 corresponds to $20MHz$ bandwidth channel, 802.11a/g/n mixed network, single spatial stream with transmission rate 60Mbps

$$w_j^l(a_0^l, a_j^l) = \frac{1 - \mathcal{X}(a_0^l, a_j^l)}{\sum_{l=1}^{L} [1 - \mathcal{X}(a_0^l, a_j^l)]}, \quad (4)$$

where $a_0^l$ denotes the profile for empty room on the $l^{th}$ WiFi device, and $\mathcal{X}(a_0^l, a_j^l)$ is the cross correlation between the profile of the empty room and the $j^{th}$ activity on the $l^{th}$ WiFi device. To reduce the computational complexity, only the CSI measurements having significant difference from the empty room profile will be included in the above calculation.

# 6. EVALUATION

In this section, we present the performance of our E-eyes system using commercial off-the-shelf WiFi devices in two apartments of different sizes.

## 6.1 Experimental Setup

### 6.1.1 Devices and Network

We conduct experiments in an 802.11n WiFi network with three off-the-shelf WiFi devices (i.e., two Lenovo T500 laptops and one Lenovo T61 laptop) connected to a single commercial wireless access point (i.e., Linksys $E2500$) in two apartments. The laptops run Ubuntu 10.04 LTS with the 2.6.36 kernel and are equipped with Intel WiFi Link 5300 cards for measuring CSI [12]. While CSI information is only publicly exposed by modified drivers for several chipsets, e.g., Intel WiFi Link 5300 and Atheros AR9390, it is internally tracked by 802.11 MIMO implementations and we expect more chipsets will expose such information in the near future. The packet transmission rate is set to $20pkts/s$. How the rate of packet transmission affects the performance will be discussed in Section 6.2.6. For each packet, we extract CSI for 30 subcarrier groups, which are evenly distributed in the 56 subcarriers of a $20MHz$ channel [3].

### 6.1.2 Apartments and Activities

We conduct experiments in two apartments of different sizes to test the generality of our system. The experimental setups in these two apartments are shown in Figure 7. The smaller one (i.e., one bedroom apartment) has the size of about 23ft $\times$ 20ft with one bedroom, one kitchen and one bathroom, whereas the larger one (i.e., two bedroom apartment) is about 24ft $\times$ 36ft with two bed rooms, one storeroom, one kitchen, one living room, and one bathroom. It is commonly accepted that the presence of manifold WiFi devices in home environments is highly possible in the near future. To name a few existing applications: smartTVs in living rooms, thermostats in bedrooms, smart-refrigerators in kitchens, and waterproof wireless speakers in bathrooms. In our experiments, one AP and three WiFi devices are placed at each apartment for daily activity monitoring.

A total of 9 typical daily in-place activities and 8 walking activities (passing through 4 door-ways) with different walking speeds are performed by 4 male adults in both apartments. These activities are listed in Table 3, and are shown in Figure 7. The yellow circles show the in-place activities, whereas the red/blue lines represent the paths of the walking activities. Due to different conditions in the two apartments (e.g., having a TV in the living room or not), we have chosen slightly different yet still typical in-place activities to perform in the two apartments. Note that we find it is typical for in-place activities to occur at dedicated locations in home environments, for example activities in a kitchen usually just occur in front of the sink or stove, beside the refrigerator, or at the dining table, whereas activities in a living room usually occur on the couch. In our experiments, the profiles were generated in one day and testing data was collected over different days. Over the days, one chair was moved to a different room, coffee makers were moved around

Actual Activity Performed

| 1-bedroom apt. | A | B | C | D | unknown | Door | Door1 | Door2 | None |
|---|---|---|---|---|---|---|---|---|---|
| A | 1 | 0 | 0 | 0 | 0 | Door1 | 1 | 0 | 0 |
| B | 0 | 1 | 0 | 0 | 0 | | | | |
| C | 0 | 0 | 0.95 | 0.05 | 0 | Door2 | 0 | 0.975 | 0.025 |
| D | 0 | 0 | 0 | 1 | 0 | | | | |
| O | 0 | 0 | 0.1 | 0 | 0.9 | None | 0 | 0 | 1 |

Identified Walking Activity & Doorway

(a) 1-bedroom apartment

Actual Activity Performed

| 2-bedroom apt. | E | F | G | H | unknown | Door | Door3 | Door4 | None |
|---|---|---|---|---|---|---|---|---|---|
| E | 1 | 0 | 0 | 0 | 0 | Door3 | 1 | 0 | 0 |
| F | 0.15 | 0.85 | 0 | 0 | 0 | | | | |
| G | 0 | 0 | 0.9 | 0.1 | 0 | Door4 | 0 | 0.875 | 0.125 |
| H | 0 | 0 | 0 | 1 | 0 | | | | |
| O | 0.05 | 0 | 0 | 0 | 0.95 | None | 0 | 0 | 1 |

Identified Walking Activity & Doorway

(b) 2-bedroom apartment

**Figure 9: Confusion matrix of walking activity identification in two different apartments.**

in the kitchen and items on tables, such as bowls and bottles, were moved, as usually occurs in daily life. Moreover, we build the profile for the empty room when there is no one at home (i.e., *Empty apartment (a)*). To test the ability of our system on differentiating diverse in-place activities that occur in the same place, we experiment with 4 in-place activities in the one-bedroom apartment: *sleeping on the bed, sitting on the bed, talking besides the sink, and washing dishes near the sink.* Furthermore, the experimenter conducts several in-place and walking activities which are not profiled (i.e., *Other activities (o)*). They are used to evaluate the robustness of our system for recognizing unknown or random activities.

### 6.1.3 Metrics

We use the following metrics to evaluate the performance of our system.

**Confusion Matrix.** Each row represents the actual activity performed by the user and each column shows the activity it was classified as by our system. Each cell in the matrix corresponds to the fraction of activity in the row that was classified as the activity in the column.

**True Positive Rate (TPR).** TPR for an activity $A$ is defined as the proportion of the instances that are correctly recognized as the activity $A$ among actual $A$ performed.

**False Positive Rate (FPR).** FPR for an activity $A$ is defined as the percentage of the instances that are incorrectly recognized as $A$ among all testing instances other than $A$.

## 6.2 Evaluation in Real Apartments

### 6.2.1 Activity Identification with Multiple WiFi Devices

Figure 8 plots the confusion matrix for the in-place activities recognition in two apartments with three WiFi devices. In the one-bedroom apartment, 7 different in-place activities (see Figure 8(a)) were performed (50 rounds for each). Another 100 rounds of different unknown in-place activities (i.e., $others$) are preformed to evaluate E-eyes's ability of detecting unknown activities. Similarly, in the two-bedroom apartment, 7 different in-place activities as shown in Figure 8(b) (each one has 50 rounds) and 100 rounds of unknown activities are performed. For the one-bedroom apartment, the average accuracy of identifying in-place activities is $97\%$ with a standard deviation of $5.66\%$ whereas in the two-bedroom apartment, the average accuracy of identifying in-place activities is $97.38\%$ with a standard deviation of $4.31\%$.

Figure 9 plots the confusion matrix for the walking activities identification and doorway passing detection in two apartments. As shown in Figure 7, $4$ trajectories for each apartment are performed, and $20$ rounds for each trajectory. Similar to that of the in-place activity experiment, we performed 20 rounds of aimless walking activities (i.e., walking in the apartment but no passing through predefined doorways) in each apartment as *others*. For the one-bedroom apartment, the average accuracy is $97\%$ when identifying these 4 walking activities. E-eyes can also achieve high accuracy of detecting doorway passing with an average accuracy of $99.17\%$. For the two-bedroom apartment, the average accuracy of identifying walking activities is $94\%$, and the passing doorway can be detected with an accuracy of $95.83\%$. The above results show that our E-eyes can distinguish a set of in-place activities and walking activities with high accuracy by using only a single WiFi access point in two apartments of different size. Our system E-eyes can thus have potential to support lots of emerging applications such as elder care, well-being management, and latchkey child safety.

### 6.2.2 Robustness Validation

We next evaluate the robustness of E-eyes by studying the false positive rates (FPRs) of identifying different activities in two apartments. Figure 10 (b) and (d) show that overall E-eyes has very low false positive rates for identifying different activities in two apartments – an average FPR of about $0.6\%$. The walking activities have higher FPRs which are around $0.8\%$ for both apartments. This is primarily because it is hard to follow exactly the same trajectory every time, and people's body movements maybe different from time to time when walking, such as the sequences of waving arms and alternating two legs. We also observe that the FPRs for identifying all activities are ranging from $0\%$ to $2.5\%$ in both apartments with an average TPR as high as $97\%$ as shown in Figure 10 (a) and (c). The results indicate that E-eyes is robust in identifying both in-place and walking activities in two apartments of different sizes.

### 6.2.3 Activity Identification with Single WiFi Device

To further show the capability of E-eyes in activity recognition with limited WiFi devices at home, we experiment with only one WiFi device connecting with one single AP. This is a challenging scenario as with only one AP and one WiFi device, the signal affected by the human body may become very weak after going through several walls. We place the WiFi device at one of the previous locations to sense the activities in both apartments. The results are shown in Figure 10. We find that E-eyes is capable of identifying activities accurately when placing a single AP at an appreciate location. In particular, Figure 10 (a) and (b) show that the TPRs of identifying both in-place and walking activities are in general over $90\%$ with FPRs less than $5\%$ in the one-bedroom apartment.

In the two-bedroom apartment, most in-place activities have TPRs over $90\%$ and FPRs less than $2\%$, except the activity *sleeping*. This is because sleeping involves little body movements and lying on the bed, thus having less effects on altering multipath environments. In addition, Figure 10 (c) and (d) show that the TPRs for walking activities $G$ and $H$ are 0 because they do not generate large moving variances and are classified as *empty room* in the pre-constructed profiles. This is because with the WiFi device and the AP separated by several walls, the conducted activities that are far away from either the WiFi device or the AP will have little effect on altering the multipath environment. Besides $G$ and $H$, the other two walking activities $E$ and $F$ still have TPRs over $90\%$ with FPRs less than $3\%$.

### 6.2.4 Distinguishing Activities in the Same Location

Given that some activities take place at the same location but with different human postures or body movements (e.g., sleeping/sitting on the bed), we experiment with such in-place activities to evalu-

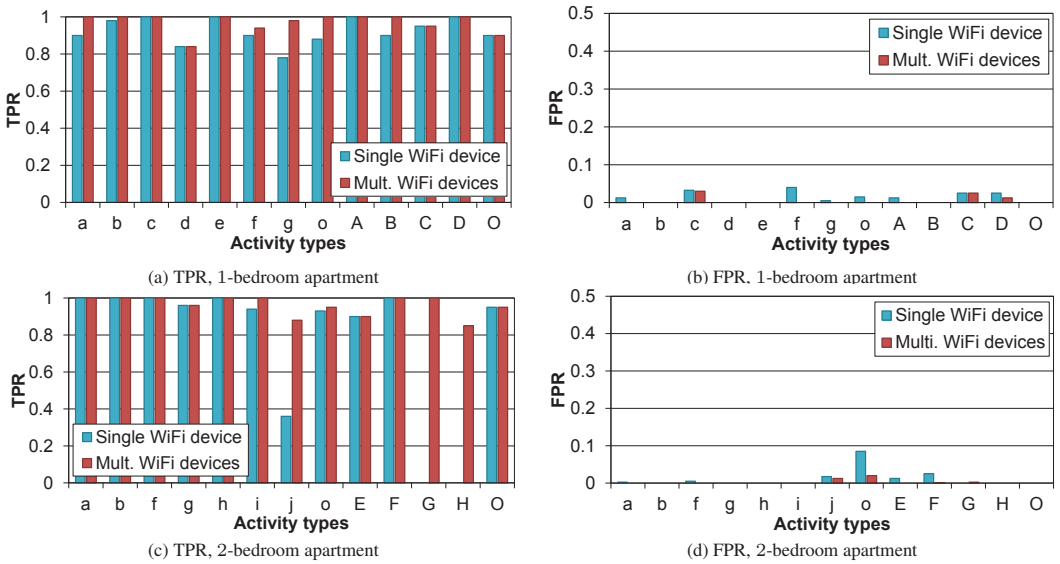


(a) TPR, 1-bedroom apartment

(b) FPR, 1-bedroom apartment

(c) TPR, 2-bedroom apartment

(d) FPR, 2-bedroom apartment

**Figure 10: True positive rate and false positive rate, in-place and walking activity recognition in two different apartments.**

ate how well E-eyes can distinguish such activities that occur in the same location. We use different numbers of EMD bins to test the impact on the resolution of identifying activities occurring in the same location. Intuitively, a larger number of EMD bins can provide more detailed distribution information. We add two more activities that occur in the same locations as two of the previously considered activities. We therefore experiment with 4 in-place activities in the one-bedroom apartment: sleeping on the *bed*, sitting on the *bed*, receiving calls nearby the *sink* and washing dishes nearby the *sink*. The system compares the measure in-place activity data against 12 profiles (the 10 from Table 3 and the two additional ones). We use the worst TPR (minimum TPR of all activity identification) and the worst FPR (maximum FPR of all activity identification), to evaluate the worst-case performance with different numbers of EMD bins. Figure 11 shows the results of identifying different activities in the same location. We find that the system can achieve high accuracy (over 97%) if the number of EMD bins is greater than 8 when different activities took place at the same locations.

### 6.2.5 *Activity Recognition Using Wider-band Signals*

Next we study the feasibility of extending E-eyes to work with wider-bandwidth channel of 802.11ac. The bandwidth of a 802.11ac channel is 4 times wider than that of 802.11n. The number of available subcarriers thus increases from 56 in 802.11n to 242 in 802.11ac. Larger numbers of subcarriers provided by 802.11ac therefore have potential to capture in-place activities more accurately and reliably. Since 802.11ac shares the same 5GHz band with 802.11n, we use multiple 802.11n channels to emulate the 802.11ac channel for CSI extraction as no handy tool is available to collect CSI from 802.11ac.

In particular, we use two laptops respectively communicating with two access points to collect CSI measurement from two 802.11n channels (40MHZ) simultaneously at the 5GHz band. The CSI measurements are off-line synchronized and cascaded in frequency domain to emulate the CSI measurements from a 802.11ac channel (80MHz). In order to make sure the two 802.11n channels share the same multipath effect, we use two external antennas for the laptops and place them next to each other. The distance between two antennas is about 2 cm, which is smaller than the half wavelength of the 5GHz WiFi signal (i.e., about 2.8cm). Similarly, we take the internal antennas of the access points out and bind them together with the distance much less than the half wavelength of the 5GHz WiFi signal. We experiment with 7 in-place activities in the two-bedroom apartment with the laptops in the living room and the access points in the kitchen as shown in Figure 7.

Figure 12 presents the performance comparison of E-eyes with the 802.11n and the emulated 802.11ac channel at 5GHz band. We find that E-eyes results in higher accuracy under the emulated 802.11ac than 802.11n, which demonstrates the feasibility of improving the recognition accuracy by utilizing wider-bandwidth of 802.11ac. The TPRs for all in-place activities are over 99%. With such high TPRs, the FPRs are still lower than 1% even for two close proximity activities *f: brushing teeth* and *g: taking a bathing*. Furthermore, comparing to the performance of the same setup using 802.11n with one WiFi device, we find that using the 802.11ac channel has about 4% improvement in the worst TPRs (i.e., increases from 94% to 98% for the activity *i: playing video game*). And the worst FPR drops to 0.67% under 802.11ac from 8.5% under 802.11n for *unknown* activities. This indicates that the wider channels (e.g., 802.11ac) can improve the recognition accuracy since it allows measurements over many additional subcarriers.

### 6.2.6 *Impact of Traffic Transmission Rate*

Since CSI is measured from each of the received packets, the higher packet transmission rate (PTR) results in larger sizes of CSI measurements for characterizing an activity. We thus study the impact of PTR on the performance of E-eyes. In particular, PTR is changed from $5pkts/s$ to $20pkts/s$ with a fixed step of $5pkts/s$. As the commercial access points send beacon signals at $10beacons/s$ to broadcast their SSID and the connection information, the range

**Table 3: Codes for in-place and walking activity profiles.**

| Code | In-place activity | Code | Walking activity |
|---|---|---|---|
| a | Empty apartment | A | Bedroom→Kitchen |
| b | Cooking | B | Kitchen→Bedroom |
| c | Eating | C | Kitchen→Bathroom |
| d | Washing dishes | D | Bathroom→Kitchen |
| e | Studying at a table | E | Outside→Bedroom1 |
| f | Brushing teeth | F | Bedroom1→Outside |
| g | Taking a bath | G | Bedroom2→Bathroom |
| h | Watching TV on a sofa | H | Bathroom→Bedroom2 |
| i | Playing video games | O | Other wandering paths |
| j | Sleeping on a bed | | |
| o | Other activities | | |

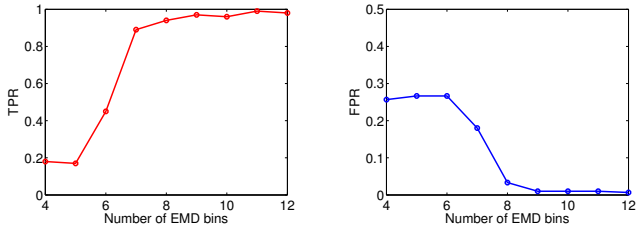


(a) (b)

**Figure 11: True positive rate and false positive rate, in worst-case with different numbers of EMD bins.**

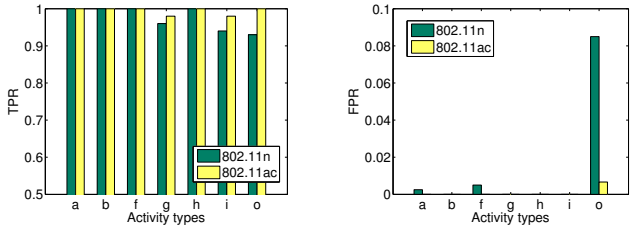


(a) True positive rate (b) False positive rate

**Figure 12: True positive rate and false positive rate of activity recognition using 802.11n or emulated 802.11ac channel.**

of our PTR is thus reasonable and includes the normal transmission rate that is considered to be energy-efficient ($10pkts/s$). Figure 13 shows the average TPRs and FPRs over all activities with different transmission rates. The increasing and decreasing trends in TPRs and FPRs respectively demonstrate that higher PTR would help to distinguish different activities. We can see that when the PTR is above 10 pkts/s, the average TPRs and FPRs are respectively over 92% and less than 2%, and the improvement of the increased packet rate is less obvious. The results demonstrate that E-eyes is capable of working with very low PTR, such as the default beacon packet rate in WiFi.

# 7. DISCUSSION

**Presence of Multiple Persons or Pets.** The current system is designed for and tested with only a single occupant. We believe that this is an important use case, particularly in an aging-in-place setting, which aims to ensure that a single person can live in his/her home and community safely and independently regardless of age and ability level. Since the temporary presence of additional people in the home can alter signatures, one improvement might be to simply detect this case using existing methods (e.g., [36]) and to suspend operation during this time. It may also be possible to switch to a different set of profiles for multiple persons. The number of profiles needed with multiple persons would increase exponentially, however. A more promising approach therefore would be to find techniques that can isolate concurrent activities in separate spaces from each other and match them against profiles separately. This would involve separating effects detected on different links and we leave this for future work. In addition, pets in the home may also change the environment dynamically. However, such cases only happen when the pet is large and moving around frequently, thus additional signal processing will be required to remove the interference in CSI and we will consider it in future work.

**Mobile Devices and Environment Changes.** E-eyes relies on stationary WiFi enabled devices, such as refrigerators, smartTVs, mounted cameras, or desktop computers. If a device is moved, our system could detect such changes by detecting many profile deviations across one link or by using other movement detection techniques (e.g., [18]) and then trigger an activity profile updating. In some cases this would require user effort. If the number of available links is large enough, however, the system might still be able to match activities using the remaining links and can automatically update the profile for the changed link. Smaller environment changes might be handled in a similar manner.

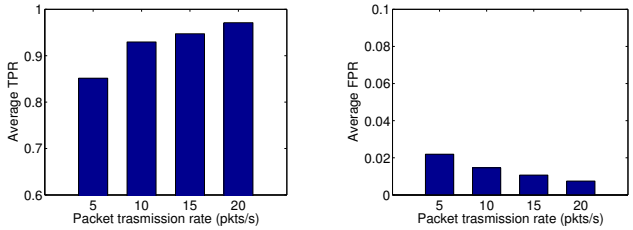


(a) Average true positive rate (b) Average false positive rate

**Figure 13: True positive rate and false positive rate of E-eyes with different PTR.**

**Constant Traffic Requirement.** The system has been evaluated with periodic traffic at various rates. When some links are in use, the system could take measurements from existing traffic and downsample to match the expected periodicity. When links are not in use, an AP-based solution could create dummy traffic on links (e.g., TCP SYNs) which invokes a response from the device. Since our system works at rates that are often used in many beaconing applications, such overhead appears manageable.

**Activities in the Same Location.** This work has exploited that many activities that are meaningful for home monitoring are linked to a few specific locations in the home, such as sinks, kitchens, couches, or desks. This has allowed us to create a limited set of profiles, which combine both location information and activity information. It is an open question to what extent a profile could be used to detect the same activity in a different location, although it is possible to create additional profiles for different locations as long as the number of activities and locations remains manageable. We also have only begun to explore to what extent it is possible to distinguish between different activities in the same location. While our results are promising, it would be useful to explore the limits of this technique by considering a larger number of different activities in the same location and the dependency of the results on the amount of change in the propagation environment.

# 8. CONCLUSION

Understanding in-home activities that persons are engaged in would facilitate a broad range of applications including wellbeing monitoring and health management. However, providing accurate activity recognition without dedicated wearable or in-building devices is challenging. We exploit the prevalence of WiFi infrastructure and design a system called E-eyes to perform device-free location-oriented activity identification by utilizing the fine-grained channel state information (CSI) available in the existing WiFi protocol (i.e., 802.11n). We find that CSI can capture the unique patterns of small-scale fading caused by different human activities at a subcarrier level, which is not available in the traditional received signal strength (RSS) extracted at the per packet level. Our system benefits from the observation that many important in-home activities occur in one or a few dedicated locations and that it is therefore often sufficient to collect a small number of profiles for these activities in each of these locations. An experiment with two pairs of activities that occur in the same location, however, also showed strong potential for the technique to identify a set of activities that occur in the same place. E-eyes applies matching algorithms to compare the CSI measurements against known profiles to identify the activity. Extensive experiments in two different-sized apartments

demonstrate that E-eyes is effective in distinguishing a number of daily activities, and that it can achieve a detection rate as high as 92% with a single AP and only one WiFi device. In addition, we also show how trends to wider-bandwidth channels (e.g., 802.11ac) will enhance activity recognition performance further.

## 9. ACKNOWLEDGEMENT

This work is supported in part by the National Science Foundation Grants CNS1217387, CNS 0845896 and IIS-1211079.

## 10. REFERENCES

[1] Familylink. http://www.familylink.net/.

[2] Leap motion. https://www.leapmotion.com.

[3] IEEE Std. 802.11n-2009: Enhancements for higher throughput, 2009. Available at http://www.ieee802.org.

[4] F. Adib, Z. Kabelac, D. Katabi, and R. C. Miller. 3d tracking via body radio reflections. In *Usenix NSDI*, 2014.

[5] F. Adib and D. Katabi. See through walls with wifi! In *ACM SIGCOMM*, 2013.

[6] M. Azizyan, I. Constandache, and R. Roy Choudhury. Surroundsense: mobile phone localization via ambience fingerprinting. In *ACM MobiCom*, 2009.

[7] P. Bahl and V. N. Padmanabhan. Radar: An in-building rf-based user location and tracking system. In *INFOCOM*, 2000.

[8] N. Banerjee and et al. Virtual compass: relative positioning to sense mobile social interactions. In *Pervasive computing*, pages 1–21. 2010.

[9] H.-l. Chang and et al. Spinning beacons for precise indoor localization. In *ACM SenSys*, 2008.

[10] E. S. Gardner. Exponential smoothing: The state of the art. *Journal of forecasting*, 4(1):1–28, 1985.

[11] A. Goswami and et al. Wigem: a learning-based approach for indoor localization. In *ACM CoNEXT*, 2011.

[12] D. Halperin and et al. Tool release: Gathering 802.11n traces with channel state information. *ACM SIGCOMM CCR*, 2011.

[13] J. Hong and T. Ohtsuki. Ambient intelligence sensing using array sensor: Device-free radio based approach. In *CoSDEO workshop*, 2013.

[14] K. Joshi, S. Hong, and S. Katti. Pinpoint: Localizing interfering radios. In *Usenix NSDI*, 2013.

[15] V. Kasteren and et. al". An activity monitoring system for elderly care using generative and discriminative models. *Personal and ubiquitous computing*, 14(6):489–498, 2010.

[16] M. Keally and et al. Pbn: towards practical activity recognition using smartphone-based body sensor networks. In *ACM SenSys*, 2011.

[17] K. Kleisouris, Y. Chen, J. Yang, and R. P. Martin. Empirical evaluation of wireless localization when using multiple antennas. *IEEE TPDS*, 21(11):1595–1610, 2010.

[18] K. Kleisouris, B. Firner, R. Howard, Y. Zhang, and R. P. Martin. Detecting intra-room mobility with signal strength descriptors. In *ACM MobiHoc*, 2010.

[19] A. E. Kosba, A. Saeed, and M. Youssef. Rasid: A robust wlan device-free passive motion detection system. In *PerCom*, 2012.

[20] J. Lei, X. Ren, and D. Fox. Fine-grained kitchen activity recognition using rgb-d. In *ACM UbiComp*, 2012.

[21] L. Li, P. Hu, C. Peng, J. Shen, and F. Zhao. Epsilon: A visible light based positioning system. In *Usenix NSDI*, 2014.

[22] H. Liu, Y. Gan, J. Yang, S. Sidhom, Y. Wang, Y. Chen, and F. Ye. Push the limit of wifi based localization for smartphones. In *ACM MobiCom*, 2012.

[23] Microsoft. X-box kinect. http://www.xbox.com.

[24] Philips. Philips lifeline. http://www.lifelinesys.com/content/.

[25] Q. Pu and et al. Whole-home gesture recognition using wireless signals. In *ACM MobCom*, 2013.

[26] L. R. Rabiner and B.-H. Juang. *Fundamentals of speech recognition*, volume 14. PTR Prentice Hall Englewood Cliffs, 1993.

[27] P. J. Rousseeuw and A. M. Leroy. *Robust regression and outlier detection*, volume 589. John Wiley & Sons, 2005.

[28] Y. Rubner and S. U. C. S. Dept. *Perceptual metrics for image database navigation*. Number 1621 in Report STAN-CS-TR. Stanford University, 1999.

[29] M. Seifeldin and et al. Nuzzer: A large-scale device-free passive localization system for wireless environments. *IEEE Transactions on Mobile Computing*, 12(7):1321–1334, 2013.

[30] S. Sen and et al. Spot localization using phy layer information. In *ACM MobiSys*, 2012.

[31] S. Sigg, S. Shi, and Y. Ji. Rf-based device-free recognition of simultaneously conducted activities. In *CoSDEO workshop*, 2013.

[32] A. Technology. Grandcare systems. http://www.grandcare.com/.

[33] G. Ten Holt, M. Reinders, and E. Hendriks. Multi-dimensional dynamic time warping for gesture recognition. In *the conference of the Advanced School for Computing and Imaging*, 2007.

[34] J. Wang and D. Katabi. Dude, where's my card?: Rfid positioning that works with multipath and nols. In *SIGCOMM*, 2013.

[35] J. Wilson and N. Patwari. Radio tomographic imaging with wireless networks. *IEEE Trans. on Mobile Computing*, 9(5), 2010.

[36] W. Xi and et al. Electronic frog eye: Counting crowd using wifi. In *INFOCOM*, 2014.

[37] J. Xiong and K. Jamieson. Arraytrack: a fine-grained indoor location system. In *Usenix NSDI*, 2013.

[38] J. Yang and Y. Chen. Indoor localization using improved rss-based lateration methods. In *IEEE GLOBECOM 2009*, 2009.

[39] J. Yang, Y. Ge, H. Xiong, Y. Chen, and H. Liu. Performing joint learning for passive intrusion detection in pervasive wireless environments. In *IEEE INFOCOM*, 2010.

[40] J. Yang, J. Lee, and J. Choi. Activity recognition based on rfid object usage for smart mobile devices. *Journal of Computer Science and Technology*, 26(2):239–246, 2011.

[41] S. Yang, P. Dessai, M. Verma, and M. Gerla. Freeloc: Calibration-free crowdsourced indoor localization. In *IEEE INFOCOM*, 2013.

[42] K. Yatani and K. N. Truong. Bodyscope: a wearable acoustic sensor for activity recognition. In *ACM UbiComp*, 2012.

[43] M. Youssef and A. Agrawala. The horus wlan location determination system. In *ACM MobiSys*, 2005.

[44] M. Youssef, M. Mah, and A. Agrawala. Challenges: device-free passive localization for wireless environments. In *MobiCom*, 2007.

[45] Y. Zhao and et al. Radio tomographic imaging and tracking of stationary and moving people via kernel distance. In *IEEE IPSN*, 2013.